Vol. 8, No. 1, 2017
ISSN 2233-4203/ e-ISSN 2093-8950
REVIEW www.msletters.org | Mass Spectrometry Letters

Application of Chemical Ionization Mass Spectrometry to Heterogeneous Reactions of OH with Aerosols of Tropospheric Interest

Jong-Ho Park[1,2]*

[1]*Nuclear Chemistry Research Division, Korea Atomic Energy Research Institute, 111 Daedeok-daero-989, Yuseong-gu, Daejeon 34057, Korea*
[2]*Department of Radiochemistry & Nuclear Nonproliferation, University of Science and Technology, 217 Gajeong-ro, Yuseong-gu, Daejeon 34113, Korea*

Received March 07, 2017; Accepted March 20, 2017
First published on the web March 31, 2017; DOI: 10.5478/MSL.2017.8.1.1

Abstract : Studies performed on heterogeneous reactions of hydroxyl radicals (OH) in aerosol materials of tropospheric interest are presented, focusing on the chemical ionization mass spectrometric approach. Kinetic investigations of these reactions reduced deviation in the estimation of OH concentration in the troposphere by atmospheric modeling from field measurements. Recently, OH uptake was investigated under wet conditions to acquire kinetic information under more realistic conditions representative of the troposphere. The information on the mechanism and kinetics of OH uptake by tropospheric aerosol materials will contribute to the updating of atmospheric models, allowing a better understanding of the troposphere.

Keywords : hydroxyl radical, heterogeneous reaction, troposphere, chemical ionization mass spectrometry, atmospheric chemistry

Introduction

The hydroxyl radical (OH) is a powerful oxidant present in the troposphere. Oxidation reactions of OH with volatile organic compounds (VOCs) are generally four to five orders of magnitude faster than those of ozone (O_3). As O_3 is five to six orders of magnitude more abundant than OH in the troposphere, the two have similar importance in terms of oxidation power.

OH is involved in numerous reactions with tropospheric constituents. One of the most important examples of its involvement is the OH-initiated oxidation of VOCs, such as aldehydes, alkanes, and alkenes, which eventually leads to their removal from the troposphere. The abundance of O_3 in the troposphere has been established mostly based on its cyclic reactions with HOx (= OH + HO_2) with indirect involvement of NOx (= NO_2 + NO).

The production of OH is initiated by the photodissociation of O_3 molecules under the effects of ultraviolet (UV) radiation, to generate electronically excited oxygen atoms followed by reaction with water vapor.

$$O_3 + h\nu\ (\lambda < 320\ nm) \rightarrow O(^1D) + O_2 \quad (1)$$

$$O(^1D) + H_2O \rightarrow 2\ OH\ (v = 1, 2, 3) \quad (2)$$

The newly formed OH is rotationally and vibrationally excited;[1-3] this process is efficiently deactivated by collision with nitrogen and oxygen molecules.[4]

Another source of OH is the fast reaction between the hydroperoxyl radical (HO_2) and nitric monoxide (NO) with a rate constant of 8.8×10^{-12} $cm^3 \cdot molecule^{-1} \cdot s^{-1}$.[5]

$$NO + HO_2 \rightarrow NO_2 + OH \quad (3)$$

Photolysis of a gaseous nitrous acid (HONO) is another source of direct OH production.

$$HONO + h\nu\ (\lambda \sim 350\ nm) \rightarrow OH + NO \quad (4)$$

The main removal sources (or "sinks") of OH in the gas phase are its reactions with carbon monoxide (CO) and methane (CH_4).[6]

$$OH + CO + O_2 \rightarrow HO_2 + CO_2 \quad (5)$$

and

$$OH + CH_4 \rightarrow CH_3 + H_2O \quad (6)$$

*Reprint requests to Jong-Ho Park
E-mail: jongho@kaeri.re.kr

$$CH_3 + O_2 + M \rightarrow CH_3O_2 + M \quad (7)$$

Although the concentration of OH ([OH]), and the contribution of each possible source to the [OH] budget, are dependent on the actinic flux and the concentrations of O_3, water vapor, NO, nitrogen dioxide (NO_2), and HONO, the global average [OH] in the troposphere ranges from several 10^5 molecules·cm^{-3} at nighttime to 5×10^6 molecules·cm^{-3} during the day.[6] OH is a short-lived radical with a lifetime of approximately 1 s under clean atmospheric conditions.[7]

Atmospheric models based on atmospheric chemistry information are used to estimate the concentrations of tropospheric species, including OH. Good agreement of models with the OH values obtained in field measurements indicates that the corresponding models represent the troposphere well. On the other hand, estimations from models deviate from measured values in cases where the models have erroneous or missing information regarding OH. Therefore, investigation of atmospheric chemistry is required to obtain more reasonable information on mechanisms and reaction kinetics regarding OH and related chemical reactions.

Investigations of OH kinetics have been performed using flow tube systems combined with various detection methods. Recently, mass spectrometry has been used to detect OH with high sensitivity, accuracy, and precision. In early studies, the ionization methods were conventional electron impact ionization or laser-induced ionization, with chemical ionization (CI) taking over later. Compared to other ionization methods, CI results in much less destructive ionization of detected species.[8-11] For CI by electron capture, a parent ion (or reagent ion), such as SF_6^-, F^-, O_2^-, and NO_2^-, encounters an OH radical in a CI region, where it transfers its electron to the OH via the following reaction

$$X^- + OH \rightarrow X + OH^- \quad (8)$$

where X^- is the parent ion. An electric field applied to a series of lenses prevents dispersal of ionized species before being introduced to a quadrupole mass analyzer. The "soft" ionization, which is specific for chemical ionization mass spectrometry (CIMS), minimizes fragmentation of the molecules resulting in enhancement of the sensitivity and simplicity of the analysis. In addition, the reaction for electron capture occurs only when the electron affinities of the species introduced to the CI region are higher than those of the parent gas species. Hence, the spectrum can be simplified by selecting the appropriate parent gas.

In the early stage, models accounted only for homogeneous reactions between OH and tropospheric constituents in the gas phase. These models estimated OH concentrations successfully in most cases. However, deviations between models and measurements were observed in some cases. This review starts from this point. Studies on the heterogeneous reaction of OH in the troposphere, performed to reduce deviation and to reinforce the atmospheric models, and the application of CIMS to atmospheric chemistry are presented. Finally, recent findings regarding the effects of wet conditions on heterogeneous OH reaction are introduced.

Discrepancy between models and field measurements of [OH] in the troposphere

Although the atmospheric models based on gas phase chemistry accurately predict OH concentrations in the troposphere, it has been reported that they still consistently overestimate the radical concentrations compared with field measurements. The overestimates ranged from 20%[12] to a factor of 4,[13] as summarized in Table 1. Such discrepancies indicate that there are missing sinks of OH that were not taken into account in the models. It has been suggested that gas phase reactions of OH with unmeasured biogenic hydrocarbons, such as isoprene type[13] and β-pinene type species,[15] may represent some of these possible missing sinks.

Heterogeneous OH reactions as additional missing sinks

In addition to gas phase reactions with unmeasured biogenic hydrocarbons, heterogeneous loss of OH in aerosol particles, which was not included in the models, has also been suggested to explain the discrepancies. Historically, no attention had been paid to heterogeneous OH reactions due to its short lifetime in the troposphere. However, heterogeneous sinks of OH can be important under certain conditions in polluted air and liquid cloud droplets. For example, Saylor *et al.* estimated that the fraction of heterogeneous loss under urban conditions would be 30% of the gas phase loss at an aerosol density of 10^5 particles·cm^{-3} and uptake coefficient of 0.1 for HO_2 (γ_{HO2}), reaching 190% at the same density and $\gamma_{HO2} = 1$, while it would be negligible at low aerosol density ($< 10^3$ particles·cm^{-3}).[17] In this case, knowledge of heterogeneous OH chemistry, such as reaction mechanisms and their rates, is required to improve the models.

Table 1. Summary of model overestimations of [OH]

Campaign	Model Overestimation of [OH]
Deuselbach (1983)[12]	20%
Fritz Peak, Colorado (1991)[13]	A factor of 4
Mauna Loa Observatory (1992)[14]	A factor of 2
Fritz Peak/Idaho Hill (1993)[15]	51%
Mace Head (1996)[16]	40%

Ironically, the heterogeneous reactions of the radicals become important even under extremely clean conditions because of slower radical sinks through gas phase reactions with organics or NOx; therefore, the contribution of heterogeneous reactions to total radical loss would be greater. The remote marine boundary layer is an example where the concentration of NOx is low and that of aerosols is moderate; under these conditions, the contribution of heterogeneous OH chemistry can be greatest.

As the first demonstration, Isaksen and Crutzen included a heterogeneous loss channel for OH and HO_2 radicals, into a photochemical model highly sensitive to HOx, using high uptake coefficient values for OH and HO_2 radicals ($\gamma_{OH} = \gamma_{HO2} = 1$).[18] However, subsequent experimental determinations of the reaction probabilities showed that these values were much smaller than unity in some cases, especially in the case of inorganic aerosols.

Despite its short lifetime in the troposphere, heterogeneous reactions of OH are now recognized as being important due to the ability to initiate oxidation of organic particulates, to react with inorganic aerosols modifying their physical and chemical properties and release photochemically active halogen products into the gas phase, and to determine cloud chemistry. At an average OH concentration of several hundredths of ppt in the troposphere, radical uptake often becomes a rate-determining step in an entire process of further physicochemical transformation of aerosol particles. Atmospheric modeling of aerosol chemistry is to a large extent constrained by the very limited kinetic data on radical uptake.

Tropospheric aerosols

The aerosols in the troposphere are fine solid or liquid particles, with particle sizes ranging from a few nanometers to tens of micrometers. They originate from natural and anthropogenic sources. Ocean wave actions and windblown mineral dust are the most important natural sources of aerosols, while combustion is an example of an anthropogenic source. The composition and amount of aerosol loading are highly dependent on the location. For example, the troposphere in an urban area normally contains high levels of organic aerosols, due to anthropogenic activities, compared to those in remote regions. Ocean-derived particles, such as sea salt aerosol, are abundant in coastal areas, while mineral dust aerosols are typically abundant in desert regions. Water droplets forming fog or clouds are also important aerosol particles in the troposphere.[6,19-20] Studies of heterogeneous OH reactions on tropospheric aerosol surfaces provide not only invaluable kinetic information to improve atmospheric models, but also allow fundamental understanding of the heterogeneous chemistry of radicals.

1. Organic aerosols

Organic aerosol particles consisting of elemental carbon (EC) and organic carbon (OC) account for the majority of tropospheric aerosols, especially in urban areas, with values of 15 – 60% by mass of aerosol particulate matter < 10 nm in diameter (PM_{10}).[21-22] OC in turn consists of primary OC emitted directly into the atmosphere and secondary OC formed by condensation of hydrocarbons through gas phase reactions onto an existing aerosol surface.[6,23] Oxidation of hydrocarbons in the gas phase by OH, O_3, or NO_2, followed by condensation on an aerosol surface, is an example of secondary OC. The amount of secondary OC also depends on the actinic flux and concentrations of pollutants. In most cases, primary OC dominates the OC budget in the troposphere, although the contribution of secondary OC increases during peaks of photochemical air pollution.

Soot, the most important particulate atmospheric carbon, is formed as a byproduct of the combustion of organic fuels and affects the climate and tropospheric chemistry. Field measurements showed that 10 – 50% of particulate matter in the troposphere is carbonaceous, with global anthropogenic emission of 12 – 24 Tg per year.[24-25] Consisting of both EC and OC, soot contains carbon atoms as the main fraction, and a small amount of hydrogen (up to 10%).

2. Mineral dust particles

Mineral dust particles originate from very specific parts of the Earth's surface, mostly from desert regions, due to the action of the wind.[26] Mineral dust particles are typically a mixture of various mineral compounds, such as silicon dioxide (silica, SiO_2), aluminum oxide (alumina, Al_2O_3), and calcium carbonate (calcite, $CaCO_3$). Due to their long lifetime, mineral dust particles can be transported long distances, spreading globally and affecting the climate and tropospheric chemistry, as well as playing an important role in cloud physics and chemistry by acting as cloud condensation nuclei (CCN). In addition, mineral dust aerosols can affect radiation balance in the atmosphere by reflecting, scattering, and absorbing incident solar light.[26-28] Another important role of mineral dust particles is to provide reaction sites for uptake of atmospheric gaseous species that are eventually involved in the following redox reactions of catalytic destruction:[29-31]

$$HO_2 + Fe(III) \rightarrow Fe(II) + O_2 + H^+ \quad (9)$$

$$HO_2 + Fe(II) + H^+ \rightarrow Fe(III) + H_2O_2 \quad (10)$$

Mineral dust particles are practically insoluble initially, even though they are hydrophilic. However, as they are exposed to the gas phase environment in the troposphere, the aerosol particles eventually become soluble by reacting with labile species, such as nitric acid (HNO_3).

Table 2. Composition of the Sea Salt Mixture[32]

Composition	Percent by Weight (%)	Density (g/L)
NaCl	58.490	24.530
$MgCl_2 \cdot 6H_2O$	26.460	5.200
Na_2SO_4	9.750	4.090
$CaCl_2$	2.765	1.160
KCl	1.645	0.695
$NaHCO_3$	0.477	0.201
KBr	0.238	0.101
H_3BO_3	0.071	0.027
$SrCl_2 \cdot 6H_2O$	0.095	0.025
NaF	0.007	0.003

3. Sea salt

Sea salt particles are released into the troposphere by ocean wave actions followed by water evaporation. Heterogeneous OH reactions on sea salt particles can play an important role in the production of halogens, such as chlorine and bromine, being responsible for their further reactions in the troposphere and the stratosphere, including O_3 destruction.

Sea salt is a mixture of different compounds. Although the composition of sea salt aerosols depends on their location of origin, the major components are sodium chloride (NaCl), magnesium chloride ($MgCl_2$), and sodium sulfate (Na_2SO_4). The typical composition of a sea salt mixture meeting American Standard for Testing Materials Standard D-1141-52-Formula A is listed in Table 2.[32]

Reaction probabilities of OH on aerosol surfaces

Hanson *et al.* measured the reaction probabilities, also called the uptake coefficient, γ, defined as the ratio of the number of gas molecules reacting with the surface to the number of gas molecules colliding with the surface, using a wetted wall flow tube and the laser-induced fluorescence (LIF) detection technique.[33]

$$\gamma = \frac{\text{number of gas molecules reacing with the suface}}{\text{number of gas molecules colliding with the surface}} \quad (11)$$

The reported γ_{OH} on pure liquid water and 28% w/w sulfuric acid (H_2SO_4) are 0.0035 at 275 K and 0.08 (lower limit) at 249 K, respectively. The room temperature value is consistent with a recent experiment by Takami *et al.*, who reported a value of 4.2 [± 2.8] × 10^{-3} at 293 K. At the same time, water ice showed higher reactivity to OH uptake.[34] Cooper *et al.* determined γ_{OH} on water ice using their low-temperature flow tube coupled to a resonance fluorescence detector.[35] The measured uptake coefficient on fresh ice was 0.1, and it decreased over time, approaching a steady-state value of 0.03.

The flow tube electron paramagnetic resonance experiment carried out by Ivanov *et al.* indicated γ_{OH} values for dry NaCl and ammonium nitrate (NH_4NO_3) of 3.2×10^{-3} at 300 K and 3.47×10^{-3} at 297 K, respectively, indicating negative temperature dependence.[36]

Table 3. The measured OH uptake coefficients for the aerosol surfaces

Surface	γ_{OH}
Liquid H_2O	0.0035,[33] 0.0042 [34]
H_2SO_4	0.08 (lower limit) [33]
Water Ice	(initial), 0.03 (steady state) [35]
$(NH4)_2SO_4$	0.03 [35]
NaCl	0.0032 [36]
NH_4NO_3	0.00347 [36]
Halocarbon wax	0.0006 [37]
Paraffin wax	0.34 [37]
Stearic-palmitic acid	0.32 [37]
Pyrene	0.32 [37]
Soot	0.88 [37]
Al_2O_3	0.20 [37]

Bertram *et al.* used a flow tube coupled with CIMS to investigate the reaction probabilities of OH on organic surfaces (halocarbon wax, paraffin wax, methyl-terminated monolayer, stearic-palmitic acid, vinyl-terminated monolayer, pyrene, soot).[37] The organic materials were shown to react efficiently with OH in hydrogen abstraction reactions. The authors also determined a γ_{OH} of 0.2 for Al_2O_3. The OH uptake coefficients for the aerosol surfaces measured in early studies are summarized in Table 3.

Heterogeneous reactions under wet conditions

Little is known regarding heterogeneous OH chemistry under actual tropospheric conditions, where water vapor is one of the major components of the troposphere, reaching up to 4% by volume. Relative humidity (RH) is defined as the ratio of the partial pressure of water (P_{H_2O}) to its saturated vapor pressure ($P^0_{H_2O}$) at a given temperature (expressed in %).

$$RH(\%) = 100 \cdot \frac{P_{H_2O}}{P^0_{H_2O}} \quad (12)$$

Due to its relatively large dipole moment (1.83×10^{-18} esu·cm) and ability to strong hydrogen bonding, water vapor can be easily adsorbed on aerosol surfaces, such as salts and dust particles, with high surface tension. For example, several studies showed that a water monolayer starts to appear on the NaCl (100) surface even at 35% RH, which is significantly below the deliquescence point of ~75%.[38] A similar value was reported by Hemminger, who showed that the first monolayer of water was completed at 20% RH, whereas multilayer water was formed efficiently above 31% RH.[39] In addition, Hemminger showed that the

adsorbed water enhances the ionic mobility on a surface at an extremely low RH of 2%. These observations suggest that heterogeneous OH reactions on aerosol surfaces can be influenced by RH over a very wide range. Therefore, for the tropospheric chemistry, it is important to determine how the heterogeneous OH reactions change under wet conditions.

However, technical problems arise in experiments at high water vapor pressure. The seeding of a sufficient amount of water vapor to achieve RH of up to 50% requires a considerable flow of carrier gas, which builds up a relatively high pressure of 100 – 200 Torr inside the flow tube reactor. Such high pressure conditions significantly slow down the fast radical uptake rate, which is mostly determined by diffusion of radicals to reactor walls.[40-42] Increasing the surface area by using a set of sub-size tube arrays or glass beads packed inside the flow tube enables simultaneous maximization of the rate of heterogeneous reaction, and minimization of diffusion limitations by decreasing the distance to reach the surface. However, a movable injector, with which flow tube systems are normally equipped to vary reaction time as described in Figure 1, is not applicable in this case.

Park *et al.* employed a parallel flow tube system to investigate heterogeneous OH reactions under wet conditions, as shown in Figure 2.[43] Two identical reactor tubes were filled with borosilicate glass beads 3 mm in diameter. The only difference between the two reactor tubes was the coating materials used; the glass beads in the reactor tube were coated with materials mimicking tropospheric aerosols, whereas those in the reference tube were coated with halocarbon wax, which is the most inert material for OH reaction.[37] With the use of two stop valves, the total flow can be switched between the reactor tube and the reference tube to compare OH uptake on reactive and inert surfaces. As the OH loss on the surfaces can be calculated by subtraction of the OH intensities from the two tubes, no movable injector is necessary. Virtual cylindrical reactor (VCR) approximation, in which a flow tube packed with beads is virtually replaced with a cylindrical reactor, as shown in Figure 3, was applied to calculate uptake constants in the conventional manner when a movable injector was used.

The reaction probabilities of OH on several organic materials (paraffin wax, pyrene, glutaric acid, and methane soot) under various RH conditions were determined as summarized in Table 4. The profile of OH uptake depends on the hydrophilicity of the surface. No changes in OH uptake by RH conditions were observed for hydrophobic organic materials (paraffin wax and pyrene). On the other hand, water adsorption on hydrophilic materials (glutaric acid and methane soot) weakened the C-H bond strength, promoting hydrogen abstraction by OH and resulting in positive dependence of OH uptake on RH.

As silica and alumina do not contain active sites for hydrogen abstraction, as seen on organic materials, heterogeneous reaction of OH on mineral dust was less favorable by a factor of two orders of magnitude compared to that on organic materials. Due to the hydrophilicity of silica and alumina, the uptake coefficient of OH showed positive dependence on RH.

Figure 4 shows the OH uptake profiles for heterogeneous reaction on the three major components of sea salt, i.e., NaCl, $MgCl_2$, and $CaCl_2$. Wet conditions did not alter OH uptake on NaCl. However, the opposite dependence of OH

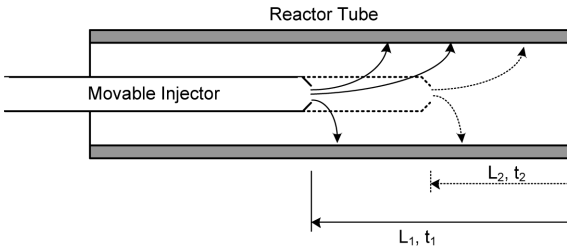

Figure 1. Schematic of a movable injector employed in kinetic studies of heterogeneous reactions. Gas-phase species of interest are effused from the end of a movable injector and react on the wall coated with the material of interest. Variable positions of the movable injector change the fraction of the wall surface corresponding to different exposed lengths (L1 and L2) or different reaction times (t1 and t2).

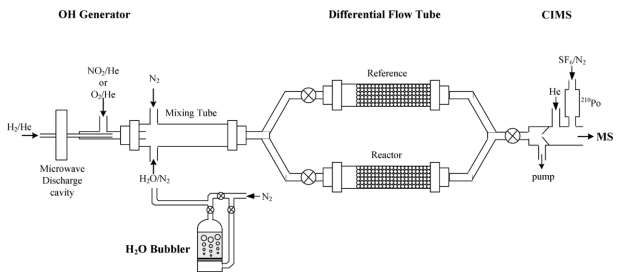

Figure 2. Schematic diagram of the parallel flow tube system.[43]

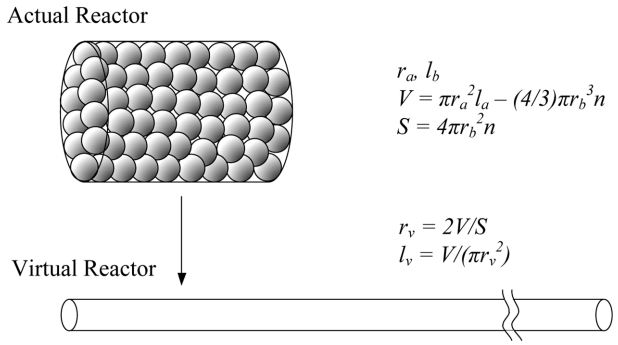

Figure 3. Schematic diagram of conversion to a virtual reactor. The virtual reactor consists of a typical cylindrical tube, while the actual reactor contains 60 beads with the same volume and coated surface area as the actual reactor.

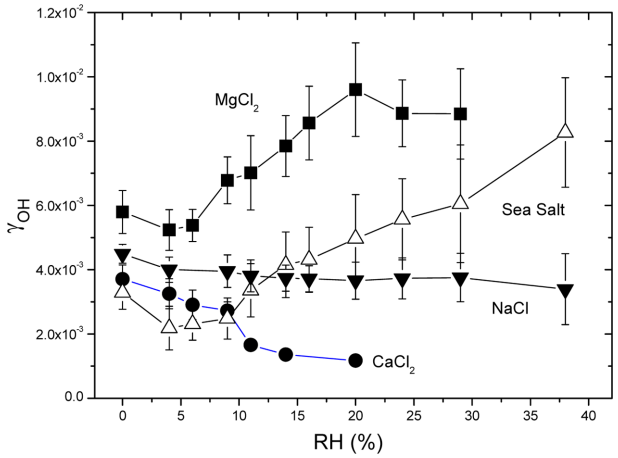

Figure 4. The dependences of γ_{OH} for NaCl, $MgCl_2$, $CaCl_2$, and sea salt on RH.

Table 4. The reaction probabilities of OH on organics under various RH conditions.[43]

RH (%)	γ_{OH}			
	Paraffin wax	Pyrene	Glutaric acid	Methane Soot
0	0.16 ± 0.03	0.30 ± 0.05	0.24 ± 0.01	0.50 ± 0.04
4	0.16 ± 0.06	0.24 ± 0.02	0.26 ± 0.01	0.36 ± 0.04
6	0.14 ± 0.04	0.25 ± 0.02	0.29 ± 0.03	0.37 ± 0.07
9	0.18 ± 0.06	0.26 ± 0.03	0.36 ± 0.02	0.30 ± 0.04
11	0.15 ± 0.06	0.29 ± 0.03	0.45 ± 0.02	0.30 ± 0.06
14	0.15 ± 0.05	0.28 ± 0.04	0.47 ± 0.06	0.32 ± 0.06
16	0.12 ± 0.04	0.31 ± 0.04	0.44 ± 0.04	0.32 ± 0.06
20	0.14 ± 0.06	0.27 ± 0.03	0.48 ± 0.02	0.34 ± 0.06
24	0.12 ± 0.07	0.24 ± 0.04	0.55 ± 0.03	0.37 ± 0.06
29	0.11 ± 0.05	0.31 ± 0.04	0.59 ± 0.03	0.40 ± 0.83
38	-[a]	0.29 ± 0.06	0.77 ± 0.05	0.44 ± 0.09
48	-[a]	-[a]	0.99 ± 0.09	0.49 ± 0.13

[a]Not measured at these RH conditions

uptake on RH was observed on $MgCl_2$ and $CaCl_2$. This can be explained by two competing effects: screening active sites for OH reaction and increasing surface acidity. Water adsorption on the salt surfaces dissociates salts into ions (i.e., Na^+, Mg^{2+}, Ca^{2+}, Cl^-, etc.), followed by redistribution of ions depending on their size—smaller ions are located closer to the surface, and vice versa.[44] Hence, cations are relocated to the surface, while Cl^- is relocated to the bulk. As chlorine ions provide active sites for heterogeneous OH reaction,[45-47] this reduces the reaction probability of OH. On the other hand, cations increase surface acidity by removal of OH^- ions (not incoming OH radicals for a heterogeneous reaction), resulting in acceleration of the rate-determining step for OH reaction.[45-47] As the latter effect is greater for Mg^{2+} than Ca^{2+}, positive dependence of OH uptake on RH was observed for $MgCl_2$, and vice versa. The water effect on OH uptake by sea salt followed patterns specific to $MgCl_2$ instead of its major constituent, NaCl. Enhancement by a factor of 2.7 in γ_{OH} for sea salt was observed at 0 – 38% RH.[43]

Summary

Atmospheric models accounting for only homogeneous reactions of OH failed to estimate the OH concentration in the troposphere in some cases, such as in urban and coastal regions. Heterogeneous reactions of OH on aerosols of tropospheric interest were considered as missing sinks of OH. This review presented studies performed on related reactions, to acquire information on reaction mechanisms and kinetics and to update the atmospheric models for better estimation of OH concentration. CIMS is widely used for these studies because of its high sensitivity and simplicity, by adoption of a soft ionization scheme and selection of an appropriate reagent gas. Recent studies on the effects of RH on OH uptake by organic materials, mineral dust, and salts were also introduced. Water adsorption on hydrophilic aerosols alters the degree of OH reaction, resulting in an increase or decrease in the reaction probability of OH. The water effect on OH uptake by sea salt followed patterns specific to $MgCl_2$ instead of its major constituent, NaCl.

The application of CIMS to the measurement of OH concentration and to the investigation of the heterogeneous reaction of OH in the troposphere has been contributing to the updating of the relating information and to the better understanding of the troposphere.

References

1. Sauder, D. G.; Stephenson J. C.; King, D. S.; Casassa, M. P. *J. Chem. Phys.* **1992**, 97, 952.
2. Park, J. -H.; Lee, H.; Kwon, H. -C.; Kim, H. -K, Choi, Y. -S.; Choi, J. -H. *J. Chem. Phys.* **2002**, 117, 2017.
3. Park, J. -H.; Lee, H.; Choi, „J. -H. *J. Chem. Phys.* **2003**, 119, 8966.
4. D'Ottone, L.; Bauer, D.; Campuzano-Jost, P.; Fardy, M.; Hynes, A. J. *Chem. Chem. Phys.* **2004**, 6, 4276.
5. Atkinson, R.; Baulch, D. L.; Cox, R. A.; Crowley, J. N.; Hampson, R. F.; Hynes, R. G.; Jenkin, M. E.; Rossi, M. J.;Troe, J. *Atmos. Chem. Phys.* **2004**, 4, 1461.
6. Seinfeld, J. H.; Pandis, S. N. *Atmospheric Chemistry and Physics.* John Wiley & Sons, Inc., New York, **1998**.
7. Heard, D. E.; Pilling, M. J. *Chem. Rev.* **2003**, 103, 5163.
8. Hanson, D. R.; Ravishankara, A. R. *J. Geophys. Res.* **1991**, 96, 5081.
9. Villalta, P. W., Huey, L. G.; Howard, C. J. *J. Phys. Chem.*, **1995**, 99, 12829.
10. Seeley, J. V.; Meads, R. F.; Elrod, M. J.; Molina, M. J. *J. Phys. Chem.* **1996**, 100, 4026.

11. Lipsion, J. B.; Beiderhase, T. W.; Molina, L. T.; Molina, M. J.; Olzmann, M. *J. Phys. Chem.* A, **1999**, 103, 6540.
12. Poppe, D.; Zimmermann, J.; Bauer, R.; Brauers, T.; Brűning, D.; Callies, J.; Dorn, H.-P.; Hofzumahaus, A.; Johnen, F. -J.; Khedim, A.; Koch, H.; Koppmann, R.; London, H.; Műller, K. –P.; Neuroth, R.; Plass-Dűlmer, C.; Platt, U.; Rohrer, F.; Rőth, E. –P.; Rudolph, J.; Schmidt, U.; Wallasch, M.; Ehhalt, D. H. *J. Geophys Res.*, **1994**, 99, 16633.
13. Eisele, F. L.; Mount, G. H.; Fehsenfeld, F. C.; Edward Marovich, J. H.; Parrish, D. D.; Roberts, J.; Trainer, M. *J. Geophys Rev.* **1994**, 99, 18605.
14. Eisele, F. L.; Tanner, D. J.; Cantrell, C. A.; Calvert, J. G. *J. Geophys. Res.* **1996**, 101, 14665.
15. Mckeen, S. A.; Mount, G.; Eisele, F.; Williams, E.; Harder, J.; Goldan, P.; Kuster, W.; Liu, S. C.; Baumann, K.; Tanner, D.; Fried, A.; Sewell, S.; Cantrell, C.; Shetter, R. *J. Geophys. Res.* **1997**, 102, 6467.
16. Carslaw, N.; Creasey, D. J.; Heard, D. E.; Lewis, A. C.; McQuaid, J. B.; Pilling, M. J.; Monks, P. S.; Bandy, B. J.; Penkett, S. A. *J. Geophys. Res.* **1999**, 104, 30241.
17. Saylor, R. D. *Atm. Environ.* **1997**, 31, 3653.
18. Isaksen, I. S.; Crutzen, P. J. *Geophys. Norvegica* **1977**, 31, 1.
19. Pandis, S. N.; Seinfeld, J. H.; Pilinis, C. *Atmos. Environ.* **1990**, 24A, 1957.
20. Wieprecht, W.; Acker, K.; Mertes, S.; Collett Jr., J.; Jaeschke, W.; Brüggermann, E.; Mőller, D.; Herrmann, H. *Atmos. Environ.* **2005**, 39, 4267.
21. Rau, J. A. *Aerosol Sci. Technol.* **1989**, 10, 181.
22. Bertram, A. K.; Ivanov, A. V.; Hunter, M.; Molina, L. T.; Molina, M. J. *J. Phys. Chem.* A **2001**, 105, 9415.
23. Pandis, S. N.; Harley, R. A.; Cass, G. R.; Seinfeld, J. H. *Atmos. Environ.* **1992**, 26A, 2269.
24. Cooke, W. F.; Wilson, J. J. N. *J. Geophys. Res.* **1996**, 101, 19395.
25. Penner, J. E.; Chuang, C. C.; Grant, K. *Clim. Dyn.* **1998**, 14, 839.
26. Prospero, J. M.; Ginoux, P.; Torres, O.; Nicholson, S. E.; Gill, T. E. *Rev. Geophys.* **2002**, 40, 1002.
27. Laskin, A.; Wietsma, T. W.; Krueger, B. J.; Grassian, V. H. *J. Geophys. Res.* **2005**, 110, D10208.
28. Vlasenko, A.; Sjogren, S.; Weingartner, E.; Stemmler, K.; Gäggeler, H. W.; Ammann, M. *Atmos. Chem. Phys.* **2006**, 6, 2147.
29. Ross, H. B.; Noone, K. J. *J. Atmos. Chem.* **1991**, 12, 121.
30. Matthijse, J.; Sedlak, D. L. *Meteorol. Atmos. Phys.* **1995**, 57, 43.
31. Dentener, F. J.; Carmichael, G. R.; Zhang, Y. ; Lelieveld, J.; Crutzen, P. J. *J. Geophys. Res.* **1996**, 101, 22869.
32. Lin, T. F.; Gilbert, J. B.; Naggar, J. A.; Imblum, T. M. *Proceedings IEEE's OCEANS'91, Honolulu, Hawaii*, **1991**. 3, 1629.
33. Hanson, D. R.; Burkholder, J. B.; Howard, C. J.; Ravishankara, A. R. *J. Phys. Chem.* **1992**, 96, 4979.
34. Takami, A.; Kato, S.; Shimono, A.; Koda, S. *Chem. Phys.* **1998**, 231, 215.
35. Cooper, P. L.; Abbatt, J. P. D. *J. Phys. Chem.* **1996**, 100, 2249.
36. Ivanov, A. V.; Gershenzon, Y. M.; Gratpanche, F.; Devolder, P.; Sawerysyn, J. –P. *Ann Geophys.* **1996**, 14, 659.
37. A. K. Bertram, A. V. Ivanov, M. Hunter, L. T. Molina, and M. J. Molina, The reaction probability of OH on organic surfaces of tropospheric interest, *J. Phys. Chem. A*, **105**, 9415-9421, 2001.
38. Peters, S. J.; Ewing, G. E. *J. Phys. Chem. B* **1997**, 101, 10880.
39. Hemminger, J. C. *Int. Rev. Phys. Chem.* **1999**, 18, 387.
40. Rudich, Y.; Talukdar, R. K.; Imamura, T.; Fox, R. W.; Ravishankara, A. R. *Chem. Phys. Lett.* **1996**, 261, 467.
41. Zasypkin, A. Y.; Grigor'eva, V. M.; Korchak, V. N.; Gershenson, Y. M. *Kinetics and Catalysis* **1997**, 38, 772.
42. Pöschl, U.; Canagaratan, M.; Jayne, J. T.; Molina, L. T.; Worsnop, D. R.; Kolb, C. E.; Molina, M. J. *J. Phys. Chem. A* **1998**, 102, 10082.
43. Park, J. –H.; Ivanov, A. V.; Molina, M. J. *J. Phys. Chem. A* **200**8, 112, 6968.
44. Knipping, E. M.; Lakin, M. J.; Foster, K. L.; Jungwirth, P.; Tobias, D. J.; Gerber, R. B.; Dabdub, D.; Finlayson-Pitts, B. J. *Science* **2000**, 288, 301.
45. Keene, W. C.; Maben. J. R.; Pszenny, A. A. P.; Galloway, J. N. *Environ. Sci. Technol.* **1993**, 27, 866.
46. Oum, K. W.; Lakin, M. J.; DeHaan, D. O.; Brauers, T.; Finlayson-Pitts, B. J. *Science* **1998**, 279, 74.
47. Finlayson-Pitts, B. J.; Hemminger, J. C. *J. Phys. Chem. A* **2000**, 104, 11463.